TUG1 as ceRNA combined with miR-29a to promotes the expression of IFITM3 in hepatocellular carcinoma

Weiwei Liu (1415150604@qq.com)
NanChang Normal University

Qian Feng
Nanchang University Second Affiliated Hospital

Wenjun Liao
Nanchang University Second Affiliated Hospital

Jun Gao
Nanchang University Second Affiliated Hospital

Jiyuan Ai
Nanchang University

Rongguiyi Zhang
Nanchang University

Enliang Li
Nanchang University Second Affiliated Hospital

Linquan Wu
Nanchang University Second Affiliated Hospital

Research

Keywords: TUG1, miR-29a, IFITM3, HCC, biological function

Posted Date: April 20th, 2020

DOI: https://doi.org/10.21203/rs.3.rs-22745/v1

Abstract

Background: Numerous studies have shown that TUG1 has an important relationship with tumorigenesis. TUG1 is highly expressed in most tumors and can promote tumor development. However, the role of TUG1 in hepatocellular carcinoma (HCC) remains to be studied. miR-29a plays a tumor suppressor role in a variety of tumors, and there is a relationship between TUG1 and miR-29a, but the specific relationship and mechanism of action are still unclear. miR-29a can inhibit the expression of IFITM3. However, the regulatory relationship between these three components requires elucidation. This study aimed to investigate the regulatory relationship between TUG1, miR-29a, and IFITM3 in human hepatocarcinogenesis.

Methods: The expression levels of TUG1 and miR-29a in tumor tissues and adjacent non-tumor tissues of 41 HCC patients were detected by real-time quantitative polymerase chain reaction. The migration and invasion of liver cancer cells were studied by a **w**ound healing assay and the Transwell method. The apoptosis rate of hepatocarcinoma cells was detected by flow cytometry, and the proliferation rate of hepatoma cells was detected by the EdU method. Immunofluorescence was selected to detect the expression of TUG1 and IFITM3 in HCC-LM3 and HL-7702. The relationship between TUG1 and miR-29a was detected using a double luciferase report and FISH. Tumors were established *in vivo* by subcutaneous injection of hepatocellular carcinoma cells into nude mice and injection of these cells into the tail vein. Western blotting was used to quantify the biomarkers.

Results: TUG1 expression increased significantly in both tumor tissues and HCC cells. The expression of miR-29a in liver cancer tissues was also significantly lower than that in normal human liver tissues. The expression of TUG1 in HCC tissue samples was negatively correlated with that of miR-29a. Moreover, the expression of TUG1 was positively correlated with the expression of IFITM3. TUG1 can regulate the migration, invasion, apoptosis, and proliferation of HCC lines *in vitro* and regulate the development of tumors *in vivo*. Knocking down TUG1 will increase miR-29a expression, and thus, weaken the invasion, migration, and proliferation of HCC cells and enhance their apoptosis. miR-29a can affect the occurrence and progression of liver cancer through IFITM3. It was found that TUG1 regulates IFITM3 in HCC cells via miR-29a, and its expression affects cell invasion, migration, proliferation, and apoptosis.

Conclusion: As a CeRNA, TUG1 competitively binds mir-29a to regulate IFITM3 and promote the development of liver cancer. Downregulation of TUG1 can significantly inhibit the migration, invasion, and proliferation of liver cancer cells, and TUG1 is expected to serve as a key gene to improve the prognosis of patients.

Background

According to the latest statistics, liver cancer is the sixth most common cancer in the world, and it is also the fourth leading cause of cancer death(1). In China, many individuals are affected by liver cancer. The most common liver cancer is hepatocellular carcinoma (HCC), which is reported to account for 75–85%

of primary liver cancers(2). Liver cancer is a fatal disease. The main treatment strategy for liver cancer is Surgical treatment and liver transplantation. but most liver cancers are diagnosed as advanced hepatocellular carcinoma,following the ideal time for treatment(3). This leads to unsatisfactory clinical efficacy and prognosis after treatment (4, 5). Therefore, it is important to elucidate the molecular mechanisms of liver cancer progression, how to diagnose liver cancer early, and to find HCC biomarkers and therapeutic targets.

Taurine up-regulated gene 1 as an important gene affecting retinal development was first proposed in 2005(6). Subsequently, lncRNAs were shown to be involved in the carcinogenic process by altering chromatin structure and acting as a small RNA sponge, Associated with expression of multiple cancer-related pathways (7, 8). Although most studies have revealed the carcinogenic effects of this lncRNA, it has also been reported that TUG1 is downregulated in non-small cell lung cancer samples, compared to non-cancer samples(9-11). In triple-negative breast cancer samples, the expression of lncRNA was reduced. Furthermore, its expression in HER2 enrichment and basal-like subtypes is higher than that of luminal subtypes(12). TUG1 also differs in expression and function in different tumors. Furthermore, its role in epithelial mesenchymal transition and activation of the Wnt/β-catenin pathway has been explored in Human cancer (11, 13). Although TUG1 has been shown to be a key factor in the progression of multiple tumors, it is unclear how its downstream target genes affect HCC progression.

Small molecule ribonucleic acid (microRNA) is an endogenous (approximately 22 nucleotides) small non-coding RNA family that can inhibit translational expression of proteins by direct binding to 3' untranslated region (3' UTR) messengers expressing the ribonucleic acid (mRNA) target gene silencing post-transcriptional regulation of gene expression(14-16). It has been reported that microRNAs are closely related to the apoptosis of nerve cells. The expression of miRNA-29a is significantly reduced in a variety of tumors (17, 18). This indicates that miR-29a is involved in a variety of tumor progression processes and plays an important role in tumor growth, metastasis, apoptosis, and proliferation(19-21). As a member of the microRNA family, miR-29a has been expressed in many tumors and has a tumor suppressor effect(22-24), but its mechanism of action in liver cancer is worthy of further study.

The interferon-inducible transmembrane protein 3 (IFITM3, also known as 18u) gene (together with IFITM1 and IFITM2) belongs to the IFITM gene family that is clustered on chromosome 11 and is also considered to be an antiviral gene(25, 26). In recent years, an increasing number of studies have found that IFITM3 expression is associated with the prognosis of a variety of tumors, such as gastrointestinal tumors and glioma, and is involved in cell migration, invasion, Proliferation, apoptosis and tumorigenesis(27-30). there are significant research value. However, the mechanism of the clinical significance of abnormal IFITM3 expression in hepatocellular carcinoma is still relatively unknown, and the upstream genes remain to be explored. This study aimed to understand how TUG1 regulates the expression of IFITM3, thereby affecting the development of HCC.

Although the research on the treatment of liver cancer is continuing, there has been no breakthrough in the treatment of advanced liver cancer. Our previous studies have shown that IFITM3 is a direct target of

mir-29a and an important gene regulating the development of liver cancer. The purpose of this study was to confirm the differential expression of TUG1 in HCC and to determine whether it regulates IFITM3 through mir-29a, thereby affecting tumor invasion, migration, proliferation, and apoptosis. The ultimate goal is to find biomarkers and therapeutic targets for early liver cancer.

Methods

Tissue specimens and microarray data

Collected forty-one pairs of histologically confirmed liver cancer and adjacent cancer specimens in the Second Affiliated Hospital of Nanchang University. The collected specimens required no chemotherapy, radiotherapy and immunotherapy. The collected specimens were immediately stored in liquid nitrogen and tissue fixation solution , The study was based on the Helsinki Declaration of 1964 and all subsequent amendments. All patients received written informed consent from the Ethics Committee of the Second Affiliated Hospital of Nanchang University. Three-hundred and seventy-four cases of liver cancer and 50 cases of normal liver tissue were accessed via the Starbase database, and the expression of TUG1 was compared.

Cell lines and cell culture

Normal liver cells (HL-7702), liver cancer cell lines MHCC-97H and HCC-LM3 were selected. All cells were purchased from Shanghai Cell Research Institute (Shanghai, China). HCC-LM3 and MHCC-97H cells were cultured in high-glucose Dulbecco's modified Eagle's medium (DMEM) containing 10% fetal bovine serum (FBS), and HL-7702 cells were cultured in RPMI 1640 medium containing 10% FBS. The cells were maintained in an incubator at 37 ℃, 5% CO_2, and 95% humidity. Cells in the logarithmic stage of growth were used.

Cell transfection

TUG1 siRNA, miR-29a inhibitor, and negative control (NC) were purchased from Guangzhou RiboBio Biotechnolog (Guangzhou). IFITM3 siRNA and NC were purchased from Shanghai Gene Pharmaceutical. MHCC-97H and HCC-LM3 cells were finally selected as the cell lines and divided into the NC group and treatment groups. Each gene interference fragment and inhibitor was transfected into cells using the Lipofectamine 3000 kit (Invitrogen; Thermo Fisher Scientific, Inc., Waltham, MA, USA). The TUG1 siRNA sequence was as follows: sense, 5' GTTGACCTTGCTGTGAGAA 3' and antisense, 5' AACCTGGGAACCTTGGATTG 3'. The miR-29a inhibitor sequence was as follows: UAACCGAUUUCAGAUGGUGCUA. The IFITM3 siRNA sequence was as follows: IFITM3-s1 sense, 5'-CCA UUC UGC UCA UCG UCA UTT-3' and antisense, 5'-AUG ACG AUG AGC AGA AUG GTT-3'.

Quantitative reverse transcription polymerase chain reaction (qRT-PCR) and western blotting

All RNA was extracted with TRIzol reagant, then reverse transcribed into cDNA using a reverse transcription kit (Takara, Tokyo, Japan), and then qRT-PCR was run using a PrimeScript RT kit (Takara). All proteins were extracted with RIPA lysate and protease inhibitor in a 100: 1 mixed liquid. The relative expression of each gene was normalized using the expression of housekeeping genes and calculated using the $2^{-\Delta Ct}$ method. The RiboBio-designed primers were TUG1, IFITM3, beta-actin. miR-29a and U6, The primary antibodies,IFITM3 (Ab109429), Bax (ab32503), Bcl2 (ab32124), tubulin (ab15246), MMP19 (ab53146), VEGFA (ab52917), N-cadherin (ab76011), and E-cadherin (ab40772) , All antibodies were purchased from Abcam. Western blotting was used to calculate the amount of protein expressed.

Scratch test

Scratch experiments to detect cell migration ability. First seed the cells into a six-well plate,. When the cells grew to 80–90% confluence, a 200-μl sterile tip was used to form a scratch in each well. Then, the separated cells were washed away with PBS, and the width of the scratches at 0 h was observed under a microscope. The cells were cultured for 24 h in new medium, Then measure the width of the scratches taken twice to calculate the ratio of cell healing The healing ratio of the scratches was calculated.

Transwell migration and invasion assays

According to the reagent instructions, the matrix glue was added, and 60–80 μl matrigel was added to the inner chamber; then, the wells were placed in the incubator for half an hour. First, a cell suspension for 12–24 h of starvation was prepared, and the cells were uniformly added to the inner chamber with or without matrigel. Then, 500 μl of serum-containing medium (DMEM) was added to each well in the outer chamber and incubation was continued for 24–48 h in the incubator. Thereafter, the cells in the chamber were washed, the cells were fixed with formaldehyde, and the outer cells were stained with 0.1% crystal violet. Finally, a picture was taken with a microscope after the water had dried.

Measurement of apoptosis via flow cytometry

The cells were cultured in suspension for 48 h and digested with trypsin without EDTA; then, flow cytometry analysis was performed using the Annexin V-FITC/PI Apoptosis Detection Kit (BD Biosciences) according to the manufacturer's instructions. Data were collected on a BD FACS Canto system and analyzed using Flow Jo software.

Cell cycle assays

The cells were cultured in suspension for 48 h, digested with trypsin without EDTA, and flow cytometry analysis was performed using a cycle kit (BD Biosciences) according to the manufacturer's instructions.

EDU assay

The cells were first seeded into a 96-well plate, then the cells were fixed, then EDU stained according to the manufacturer's instructions (RiboBio), and finally observed and photographed under a fluorescence

microscope.Blue represents all cells, red represents proliferating cells, and the EdU positive rate indicates the ratio of red cells to blue cells.

In vivo experiment

Adult male nude mice of 6-8 weeks were selected as experimental objects and purchased from Hunan SJA Experimental Animal Co., Ltd. (Hunan, China). Nude mice were injected with a phosphate solution containing 1×10^7 cells. Tumor volume was measured with calipers every 4 days: tumor volume = (shortest diameter 2 × longest diameter) / 2. After 4 weeks of photographing, the mice were anesthetized, the tumors were collected and weighed, and the expression of IFITM3 in the subcutaneous tumors was detected by immunohistochemistry, qRT-PCR, and western blotting. To assess lung metastasis, a phosphate solution containing 1×10^6HCC-LM3 was injected into the tail vein of nude mice. Three weeks later, the mice were sacrificed after anesthesia, and nude mice lung tissues were taken for hematoxylin and eosin (H & E) staining and immunization.

Hematoxylin & eosin and immunohistochemical staining

The prepared tissue was fixed with a Tissue fixation fluid, placed in a paraffin block, and cut into paraffin sections. Dewaxing was first carried out with xylene, and then the tissue sections were dehydrated with gradient alcohol. Sections were stained with H&E to determine if their morphology changed and then rehydrated and microwaved in sodium citrate buffer (10 mmol/L, pH 6.0) to restore the antigen. Sections were incubated with 0.3% hydrogen peroxide/phosphate buffered saline for 30 min and then blocked with serum. Subsequently, tissues were incubated with a 1:200 dilution of rabbit monoclonal antibody IFITM3 (ab15592, Abcam, Cambridge, MA, USA) at 4°C overnight. Wash 3 times with phosphate buffered saline (PBS) every 5 minutes, and drop the secondary antibody at 37 ° C for 30 minutes. Next, the sections were stained with diaminobenzidine (DAB) and hematoxylin dye, then the excess dye was rinsed with running water, then rehydrated with gradient alcohol, and sealed with neutral resin. Finally, observe and take pictures under the microscope.

Dual-luciferase reporter assay

The dual-luciferase reporter assay (DR) has become an effective means to study the involvement of transcription factors in gene regulation. By analyzing the DNA fragment of the promoter, the transactivation ability of the promoter-binding element is verified, and transcription is investigated. The molecular mechanism of the factor in signal transduction can be observed since the miRNA acts mainly through the 3' UTR on the target gene, and the 3' UTR region of the target gene can be constructed behind the reporter gene luciferase, by comparing or overexpressing the miRNA. Reporter gene expression changes (monitoring changes in luciferase activity) can quantitatively reflect the inhibitory effect of miRNA on the target gene, combined with site-directed gene mutations and other methods to further determine the site of action of the miRNA and the target gene 3' UTR. Dual luciferase reporter assays were used to determine if miR-29a is a direct target gene for TUG1.

FISH assay

Fluorescence in situ hybridization (FISH) is sensitive, accurate, and can detect multiple genes at a time. It can be used to determine the exact position of the target gene, the positional relationship between several genes, and the relationship between genes and telomeres. The relationship between genes and centromeres is an essential element in the construction of genetic maps. The nucleus stained by DAPI is blue under the excitation of ultraviolet light, and the positive expression is the corresponding fluorescein-labeled fluorescence. FAM (488) is green and cy3 is red. In situ hybridization of mRNA showed that the results were positive for the cytoplasm, and a few positive nuclear results were normal. There were different expression levels of microRNA and lncRNA. The fluorescence intensity was different depending on the amount of expression. The TUG1 probe used was as follows: 5'-DIG-AATCTACCTCCAGTGTTCCTGCCGCATCGTG-DIG-3'. The miR-29a-3p probe used was as follows: 5'-DIG-TAACCGATTTCAGATGGTGCTA-DIG-3’.

Immunofluorescence assay:

By combining the antibody with some tracer substances, the antigen-antibody reaction is used to locate the antigenic substance in the tissue or cell. Immunofluorescence steps include, cell fixation and permeation, blocking, incubation of primary antibodies, secondary antibodies, etc. Immunofluorescence can localize the expression of TUG1 and IFITM3 whether it is intranuclear or extranuclear.

Statistical Analysis.

Statistical analysis software using GraphPad Prism 7.0 and SPSS 22.0.The expression of TUG1 in HCC tissues and adjacent tissues was compared using the Wilcoxon paired test. The correlation between TUG1 and miR-29a expression levels was found to be statistically significant using Spearman correlation analysis. Differences in overall survival were assessed using the log rank (Mantel Cox) test. The t-test was used to analyze the difference in expression of tumor tissues and paracancerous tissues. The chi-square test was used to compare the data from the two groups. Considered statistically significant when p-value is less than 0.05.

Results

1.The difference in expression of TUG1 in HCC

To evaluate TUG1 expression differences, we performed qRT-PCR in 41 HCC tissues and adjacent non-tumor tissues, and performed qRT-PCR in multiple HCC cell lines and normal liver cells (HL-7702).confirming that TUG1 was significantly upregulated in HCC cell lines and tissues (Figure. 1A, 1B),This is consistent with the results we found in the database (Figure. S1A) .It was also found by Immunofluorescence that the expression of TUG1 was significantly higher in HL-LM3 cells than in HL-7702 cells (Figure. 1C). We found through the qRT-PCR results and prognosis follow-up that the higher the TUG1 expression level, the worse the prognosis of the patients (Figure. 1D). This is consistent with the

results we found in the database (Figure. S1C). And we found through the database that TUG1 expression is closely related to tumor grade (Figure. S1D).

2. Downregulation of TUG1 inhibits invasion, migration, proliferation, and apoptosis of HCC cells

To investigate the role of TUG1 in HCC, we first transfected TUG1SiRNA into HCC-LM3 and MHCC-97H cells and then examined the expression of TUG1 mRNA (Figure. 2A). We speculated that TUG1 plays a role in cancer promotion in HCC cells, and this was validated in functional experiments. The scratch experiments showed that downregulation of TUG1 reduced cell transfer capacity (Figure. 2B). The Transwell method showed that downregulation of TUG1 reduced cell invasion and migration (Figure. 2C). The EdU method demonstrated that downregulation of TUG1 reduced cell proliferation (Figure. 2D). Flow cytometry showed an increase in the rate of apoptosis in HCC cells after downregulation of TUG1 (Figure. 2E). In the cycle detection, the proportion of cells in G1 increased after downregulating TUG1 (Figure. 2F). We also tested related proteins to further demonstrate our conclusions (Figure. 2G). Therefore, we believe that downregulation of TUG1 can inhibit HCC cell invasion, migration, and proliferation and promote apoptosis.

3. The relationship between TUG1 and miR-29a

We found a possible link between TUG1 and miR-29a through multiple database comparisons (Figure. 3A, 3B). Next, we obtained the miR-29a expression in liver cancer specimens by qRT-PCR (Figure. 3C) and constructed a scatter plot with the expression of TUG1 (Figure. 3D).This result is consistent with what we found in the database (Figure. S1B).The results showed that there was a negative correlation between the two. Next, We proved that miR-29a is a target gene of TUG1 through double luciferase report and FISH detection (Figure. 3E, 3F).

4. TUG1 regulates miR-29a in HCC cells

To investigate the interaction of TUG1 and miR-29a in HCC, we first transfected TUG1SiRNA and miR-29a inhibitors into HCC-LM3 and MHCC-97H cells and then detected the expression of miR-29a mRNA. We hypothesized that TUG1 is negatively correlated with miR-29a. TUG1 could reverse-regulate miR-29a (Figure. 4A), and this was verified via functional experiments. The scratch test demonstrated that downregulation of TUG1 reduced cell transfer capacity, while downregulation of miR-29a enhanced cell transfer capacity (Figure. 4B). The Transwell method was used to demonstrate that downregulation of TUG1 reduced cell invasion and migration, whereas downregulation of miR-29a was reversed (Figure. 4C). The EdU method proved that downregulation of TUG1 reduced cell proliferation, while downregulation of miR-29a resulted in the opposite effect (Figure. 4D). Flow cytometry demonstrated that the opposite results (Figure. 4E, 4F) were also observed with regard to the downregulation of apoptosis and the cell cycle in cells showing TUG1 and miR-29a downregulation. We also ran related proteins to further validate our results (Figure. 4G). In addition, our luciferase reporter demonstrated that miR-29a is the target gene for TUG1. Therefore, we conclude that TUG1 can inhibit the expression of miR-29a.

5. TUG1 regulation of IFITM3 in HCC cells

Our previous studies showed that miR-29a can reverse-regulate IFITM3. We speculate that TUG1 can positively adjust IFITM3. Next, we made a diagram showing the relationship between TUG1 and IFITM3 expression using the results of qRT-PCR (Figure. S1E). We found through qRT-PCR that IFITM3 also decreases when TUG1 is downregulated (Figure. 5A). Next, we validated our hypothesis through functional experiments. The scratch test demonstrated that a reduction of TUG1 and IFITM3 expression would reduce the cell transfer capacity (Figure. 5B). Transwell experiments showed that down-regulating IFITM3 and TUG1 reduced cell infiltration and metastasis capacity (Figure. 5C); EdU analysis showed that down-regulating IFITM3 and TUG1 decreased cell proliferation capacity (Figure. 5D). Down-regulating the expression of IFITM3 and TUG1 increased the level of apoptosis (Figure. 5E) and inhibited proliferation (figure. 5F). We also used western blots to further validate our results (Figure. 5G). Therefore, we believe that TUG1 can positively regulate IFITM3.

6. miR-29a regulates IFITM3 in HCC cells

To investigate the interaction of miR-29a with IFITM3 in HCC, we detected changes in mRNA and protein levels of IFITM3 after 36 h due to transfection of inhibitors of miR-29a and Si-IFITM3. We found that IFITM3 mRNA and protein levels were elevated (Figure. 6A) after transfection of miR-29a inhibitors. Therefore, we suspect that miR-29a can inhibit the expression of IFITM3. Next, we validated our hypothesis through functional experiments. We found that the scratch test demonstrated that downregulation of miR-29a enhanced the ability of both cells to metastasize, and downregulation of IFITM3 reduced cell transfer capacity (Figure. 6B). Transwell experiments showed that downregulation of miR-29a cell invasion and migration ability was also enhanced, while downregulation of IFITM3 showed the opposite effects (Figure. 6C). EDU detection showed that downregulation of miR-29a enhances cell proliferation, and downregulation of IFITM3 reduces cell proliferation (Figure. 6D). Flow cytometry showed that down-regulation of miR-29a inhibited apoptosis, while down-regulation of IFITM3 promoted apoptosis, and down-regulation of cell cycle assessment also showed opposite results (Figure. 6E, 6F). We further confirmed our conjecture (Figure. 6G) by western blotting. Therefore, we believe that miR-29a can negatively regulate IFITM3.

7. TUG1 regulates IFITM3 through miR-29a in HCC cells

To investigate the relationship between the three factors, we first determined that TUG1 can negatively regulate miR-29a (Figure. 4), then that TUG1 can positively regulate IFITM3 (Figure. 5), and finally the relationship between miR-29a and IFITM3 (Figure. 6). Immunofluorescence analysis then showed that IFITM3 was highly expressed in HCC-LM3 compared to HL-7702(Figure. 7A). Therefore, we divided the experimental components into six groups, namely transfected Si-Nc, si-TUG1, miR-29a inhibitor, Si-IFITM3, Si-TUG1 + miR-29a inhibitor, and miR-29a inhibitor + Si -IFITM3. After 36 h, the mRNA and protein levels of IFITM3 were examined. We found that the downregulation of TUG1 and IFITM3 decreased the mRNA and protein levels of IFITM3, which increased after downregulation of miR-29a. After down-regulating TUG1 and miR-29a, and down-regulating miR-29a and IFITM3, the expression of IFITM3 mRNA

and protein was not different from that of the NC group. (Figure. 7C, 7D). Therefore, we found that TUG1 promotes the expression of IFITM3 by inhibiting the expression of miR-29a. Therefore, we concluded that TUG1 regulates IFITM3 via miR-29a, thereby affecting the development and progression of HCC(Figure. 7B).

8. *In vitro* experiments

To investigate the effects of TUG1 and miR-29a in vivo, we subcutaneously injected TUG1 knockdown cells, miR-29a knockout cells, or control cells into nude mice, and then evaluated the tumor growth. The tumor growth rate of nude mice in the TUG1 down-regulated group was significantly slower than that in the control group and the nude mice group that down-regulated TUG1 and miR-29a at the same time (Figure. 8A); the final size and weight of the tumor were also smaller than those in case of the other two groups (Figure. 8B, 8C). Next, we assessed the relationship between TUG1 and miR-29a *in vivo*. The immunohistochemical results showed that knocking down TUG1 significantly reduced the average area of IFITM3 immune-positive tumors (Figure. 8D). The lung metastasis test showed that the degree of tumor metastasis and the average area of IFITM3 immune-positive lung tissue were significantly reduced after knocking down TUG1, while knocking down TUG1 and miR-29a at the same time resulted in findings similar to those of the control group (Figure. 8E, 8F). In addition, by examining tumor tissue using qRT-PCR and western blotting (Figure. 8G, 8H), we found that the expression of IFITM3 in tumor tissues of mice with TUG1 knockdown was significantly lower than that of the other two groups. These results indicate that TUG1 is able to influence the miR-29a-mediated regulation of IFITM3 to promote tumor development *in vivo*.

Discussion

This study first proposes that TUG1 plays an important role in HCC as an oncogene and competitively binds to miR-29a as a CeRNA to regulate IFITM3, which in turn affects the development and progression of liver cancer.

In recent years, with the development of bioinformatics and the development of high-throughput sequencing, long-chain non-coding RNA has received an increasing amount of attention. lncrna is an RNA that is more than 200 nucleotides in length and lacks the ability to encode a protein(10, 31, 32). TUG1 is a new type of cancer-related lncRNA, which is abnormally expressed in various types of cancer, and has the function of oncogenes or tumor suppressor genes(9, 32, 33). The biological functions of TUG1 in different tumors vary widely. TUG1, as an lncRNA, plays an important role in many tumors, but its specific mechanism of action in liver cancer has not been studied. The results of qRT-PCR showed that the expression of TUG1 in liver cancer tissues and cells was significantly higher than that in adjacent tissues and normal hepatocytes. We found that the expression of TUG1 in liver cancer cells (HCC-LM3) was significantly higher than that in normal cells and hepatocytes (HL-77O2), which is consistent with the previously reported results. Next, we carried out biological function experiments by transfecting TUG1 SiRNA and found that downregulation of TUG1 can reduce the invasion, metastasis, and proliferation and

enhance apoptosis of HCC cells. In our prognostic follow-up analysis, The survival time of patients with high expression of TUG1 was significantly shorter than that of patients with low expression. It can be seen that TUG1 plays an important role as an oncogene in liver cancer. TUG1 is expected to be a biomarker and therapeutic target for the diagnosis and prognosis of liver cancer.

MicroRNAs play an important role in the occurrence and pathological processes of various tumors. As a member of the micro RNA family, miR-29a plays an important role in HCC. Our previous studies have shown that miR-29a can inhibit the biological functions of liver cancer cells such as metastasis, invasion, and proliferation(15, 17, 20). Additionally, its expression has a close relationship with tumor TNM staging, multifocal tumors, and venous invasion. After downregulating miR-29a in HCC cells, we found that the translocation, invasion, and migration of HCC-LM3 and MHCC-97H cells increased, their proliferative ability was enhanced, and their apoptosis ability was weakened. This is consistent with our previously reported results, and it also verified that miR-29a acts as a tumor suppressor gene to control the occurrence and development of tumors(34). We found that TUGI was negatively correlated with the expression of miR-29a by data alignment. We also found that TUG1 was highly expressed in our liver cancer samples using qRT-PCR, while miR-29a was highly expressed in HCC. The higher the TUG1 expression, the lower the expression of miR-29a. We used immunofluorescence and dual luciferase to show that miR-29a is a downstream target gene of TUG1. In recent years, TUG1 has been found to act as a microRNA (miRNA) sponge to indirectly regulate the expression of miRNA target genes and plays a leading role in the progression of various cancers. However, it is unclear how the combination of TUG1 and miRNA affects the progression of liver cancer. The main objective of this experiment was to study the involvement of TUG1 and miR-29a in the progression of HCC.

In the Asian population, IFITM3 rs12252 is associated with the severity of influenza infection. However, in recent years, there has been growing evidence that IFITM3 is closely related to the development and prognosis of many tumors(28, 30). For example, Li et al Studies show that expression is significantly up-regulated in colon cancer and has an important relationship with its development and metastasis(27). Andreu et al Studies have shown that IFITM3 is significantly overexpressed in the rectum and can rapidly induce activation of the β-catenin signaling pathway(35). In esophageal squamous cell carcinoma, patients with high expression of IFITM3 are more likely to develop lymph node metastasis after surgery. Downregulation of IFITM3 expression inhibits breast cancer cell growth and colony formation. In liver cancer, IFITM3 can promote tumor metastasis, and patients with high expression of IFITM3 have a relatively poor prognosis. Therefore, IFITM3 has been shown to play a key role in tumorigenesis. Our previous studies have shown that IFITM3 can be regulated by miR-29a and bind to the regulator of TUG1 and miR-29a. We first proposed that TUG1 affects the expression of IFITM3 by regulating miR-29a, which in turn affects the occurrence and development of HCC.

TUG1, miR-29a, and IFITM3 all have a significant relationship with the occurrence and progression of various tumors, but whether there is a relationship between the three is still unclear. The main goal of this study was to explore the effects of the three factors on liver cancer. First, multiple databases were used to detect the expression of TUG1, miR-29a, and IFITM3 in HCC tissues. We found that overexpression of

TUG1 and IFITM3 and non-overexpression of miR-29a may affect the prognosis of patients. We then verified the expression of the three factors in cell lines. We found that after downregulating TUG1, miR-29a expression was upregulated and IFITM3 expression was downregulated. This result indicates that TUG1 may regulate IFITM3 by regulating the expression of miR-29a. Next, we verified our results in a functional test. It was concluded that TUG1 can regulate IFITM3 through miR-29a, which in turn affects invasion, metastasis, and proliferation of HCC. Finally, we further confirmed our results in animal experiments. Therefore, TUC1- and IFITM3-overexpressing HCC and miR-29a-non-overexpressing HCC may be more aggressive and more malignant, and such patients are more prone to multifocal and intrahepatic recurrence of tumors.

In conclusion, the results of this experiment suggest that TUG1 can regulate IFITM3 through miR-29a, which in turn affects the occurrence and development of HCC. This study aims to further elucidate the molecular mechanism of liver cancer, and hope to provide a new therapeutic target for the diagnosis and treatment of liver cancer.

Conclusions

Combined with the data provided in this study: TUG1 is a tumor-promoting gene of HCC, Down-regulation of TUG1 can significantly inhibit the growth and metastasis of HCC cells, and the expression of TUG1 is closely related to the prognosis of HCC. In addition, TUG1 can be used as a ceRNA to competitively bind miR-29a to regulate the expression of IFITM3, thereby affecting the occurrence and development of HCC. In summary, TUG1 is very likely to be a potential therapeutic target for HCC, which can provide a new direction for the treatment of HCC.

Abbreviations

TUG1: Taurine up-regulated gene 1; miR-29a:microRNA 29a; IFITM3: The interferon-inducible transmembrane protein 3; HCC: hepatocellular carcinoma; qRT-PCR: Quantitative real-time PCR; DR: Dual-luciferase reporter; FISH: Fluorescence in situ hybridization.

Declarations

Acknowledgments

We would like to express our sincere gratitude to the staff and managers of the Molecular Medicine Laboratory of the Second Affiliated Hospital of Nanchang University of Jiangxi for the experimental facilities provided.

Funding

This research was funded by the National Natural Science Foundation of China (N0.81860431), the Natural Science Foundation of Jiangxi Province (NO.20181BBG70025), and the project of the Jiangxi

Provincial Health and Health Committee (NO.20204266).

Availability of data and materials

The datasets used and analysed during the current study are available from. the corresponding author on reasonable request.

Authors' contributions

WL and LW conceived and designed the study. WL, QF and EL participated in the data acquisition.WL, JG and JA analyzed and interpreted the data.WL,RZ,EL wrote, reviewed and / or revised the manuscript. LW and ELwere in charge of the study. WL, QF and WL contribute equally for this study and were considered as the co-first author, EL and LW are considered co-corresponding authors.

Ethics approval and consent to participate

All experiments strictly followed the panel's specific guidelines for animal feeding, treatment, and euthanasia. All animal experiments were approved by the Animal Experiment Ethics Committee of the Second Affiliated Hospital of Nanchang University, and all were implemented strictly in accordance with the "Guidelines for the Care and Use of Laboratory Animals."

Consent for publication

All authors have read and agreed to the publication of the final manuscript.

Competing interests

The authors declare no conflicts of interest in this work.

References

1. A R, V DR, A S, M R, G M, P L, et al. Carcinogenesis and Metastasis in Liver: Cell Physiological Basis. Cancers. 2019;11(11):undefined.
2. XD Z, HC S. Emerging agents and regimens for hepatocellular carcinoma. Journal of hematology & oncology. 2019;12(1):110.
3. He Y, Li M, Wujisiguleng, Lv B, Huan Y, Liu B, et al. Array. Biosci Rep. 2018;38(6).
4. M B, N M, AR H, El C, JC N. Systemic Treatment for Advanced Hepatocellular Carcinoma. Liver cancer. 2019;8(5):341-58.
5. S B, JA M, AG S. Review article: new therapeutic interventions for advanced hepatocellular carcinoma. Alimentary pharmacology & therapeutics. 2019;undefined(undefined):undefined.
6. EB Z, DD Y, M S, R K, XH L, LH Y, et al. P53-regulated long non-coding RNA TUG1 affects cell proliferation in human non-small cell lung cancer, partly through epigenetically regulating HOXB7 expression. Cell death & disease. 2014;5(undefined):e1243.

7. Qian W, Ren Z, Lu X. Knockdown of long non-coding RNA TUG1 suppresses nasopharyngeal carcinoma progression by inhibiting epithelial-mesenchymal transition (EMT) via the promotion of miR-384. Biochem Biophys Res Commun. 2019;509(1):56-63.
8. Qin J, Bao H, Li H. Correlation of long non-coding RNA taurine-upregulated gene 1 with disease conditions and prognosis, as well as its effect on cell activities in acute myeloid leukemia. Cancer Biomark. 2018;23(4):569-77.
9. Tang L, Ding J, Liu Z, Zhou G. LncRNA TUG1 promotes osteoarthritis-induced degradation of chondrocyte extracellular matrix via miR-195/MMP-13 axis. Eur Rev Med Pharmacol Sci. 2018;22(24):8574-81.
10. Tang T, Cheng Y, She Q, Jiang Y, Chen Y, Yang W, et al. Long non-coding RNA TUG1 sponges miR-197 to enhance cisplatin sensitivity in triple negative breast cancer. Biomed Pharmacother. 2018;107:338-46.
11. Yang Y, Sun D, Yu J, Zhang M, Yi C, Yang R, et al. Long noncoding RNA TUG1 promotes renal cell carcinoma cell proliferation, migration and invasion by downregulating microRNA-196a. Mol Med Rep. 2018;18(6):5791-8.
12. G Y, H Z, W Y, L M, B L. lncRNA TUG1 Promotes Cisplatin Resistance by Regulating CCND2 via Epigenetically Silencing miR-194-5p in Bladder Cancer. Molecular therapy Nucleic acids. 2019;16(undefined):257-71.
13. Zhang L, Yu S, Wang C, Jia C, Lu Z, Chen J. Establishment of a non-coding RNAomics screening platform for the regulation of KRAS in pancreatic cancer by RNA sequencing. Int J Oncol. 2018;53(6):2659-70.
14. C H, L W, H S, C W. inhibits the progression of oral squamous cell carcinoma by targeting Wnt/β-catenin signalling pathway. Artificial cells, nanomedicine, and biotechnology. 2019;47(1):3037-42.
15. K W, J Y, B W, H W, Z S, G L. miR-29a Regulates the Proliferation and Migration of Human Arterial Smooth Muscle Cells in Arteriosclerosis Obliterans of the Lower Extremities. Kidney & blood pressure research. 2019;44(5):1219-32.
16. Li Y, Liu Y, Zhou X, Chen S, Chen X, Zhe J, et al. MiR-29a regulates the proliferation, aromatase expression, and estradiol biosynthesis of human granulosa cells in polycystic ovary syndrome. Mol Cell Endocrinol. 2019;498:110540.
17. Lian W, Ko J, Chen Y, Ke H, Hsieh C, Kuo C, et al. MicroRNA-29a represses osteoclast formation and protects against osteoporosis by regulating PCAF-mediated RANKL and CXCL12. Cell Death Dis. 2019;10(10):705.
18. Liao B, Zhou M, Zhou F, Luo X, Zhong S, Zhou Y, et al. Exosome-Derived MiRNAs as Biomarkers of the Development and Progression of Intracranial Aneurysms. J Atheroscler Thromb. 2019.
19. Liao Y, Ouyang L, Ci L, Chen B, Lv D, Li Q, et al. Pravastatin regulates host foreign-body reaction to polyetheretherketone implants via miR-29ab1-mediated SLIT3 upregulation. Biomaterials. 2019;203:12-22.

20. Razavi T, Kouhsari S, Abnous K. Morin Exerts Anti-Diabetic Effects in Human HepG2 Cells Via Down-Regulation of miR-29a. Exp Clin Endocrinol Diabetes. 2019;127(9):615-22.
21. RW W, WS L, YS C, CW K, HC K, CK H, et al. MicroRNA-29a Counteracts Glucocorticoid Induction of Bone Loss through Repressing TNFSF13b Modulation of Osteoclastogenesis. International journal of molecular sciences. 2019;20(20):undefined.
22. X C, R W, T J, H D. Notoginsenoside R1 alleviates TNF-α-induced pancreatic β-cell Min6 apoptosis and dysfunction through up-regulation of miR-29a. Artificial cells, nanomedicine, and biotechnology. 2019;47(1):2379-88.
23. Xu W, Li Z, Zhu X, Xu R, Xu Y. miR-29 Family Inhibits Resistance to Methotrexate and Promotes Cell Apoptosis by Targeting COL3A1 and MCL1 in Osteosarcoma. Med Sci Monit. 2018;24:8812-21.
24. Xue X, Zhao Y, Wang X, Qin L, Hu R. Development and validation of serum exosomal microRNAs as diagnostic and prognostic biomarkers for hepatocellular carcinoma. J Cell Biochem. 2019;120(1):135-42.
25. Appourchaux R, Delpeuch M, Zhong L, Burlaud-Gaillard J, Tartour K, Savidis G, et al. Functional Mapping of Regions Involved in the Negative Imprinting of Virion Particle Infectivity and in Target Cell Protection by Interferon-Induced Transmembrane Protein 3 against HIV-1. J Virol. 2019;93(2).
26. B Z, H W, G Z, P L. The role of IFITM3 in the growth and migration of human glioma cells. BMC neurology. 2013;13(undefined):210.
27. D L, Z P, H T, P W, X K, D Y, et al. KLF4-mediated negative regulation of IFITM3 expression plays a critical role in colon cancer pathogenesis. Clinical cancer research : an official journal of the American Association for Cancer Research. 2011;17(11):3558-68.
28. D W, H L-S, A A-H, T D. IFITM3: How genetics influence influenza infection demographically. Biomedical journal. 2019;42(1):19-26.
29. Hensen L, Matrosovich T, Roth K, Klenk H, Matrosovich M. Hemagglutinin-dependent tropism of H5N1 and H7N9 influenza viruses to human endothelial cells is determined by reduced stability of the HA which allows the virus to cope with inefficient endosomal acidification and constitutively expressed IFITM3. J Virol. 2019.
30. Manjunath S, Saxena S, Mishra B, Santra L, Sahu A, Wani S, et al. Early transcriptome profile of goat peripheral blood mononuclear cells (PBMCs) infected with peste des petits ruminant's vaccine virus (Sungri/96) revealed induction of antiviral response in an interferon independent manner. Res Vet Sci. 2019;124:166-77.
31. Shao H, Dong D, Shao F. Long non-coding RNA TUG1-mediated down-regulation of KLF4 contributes to metastasis and the epithelial-to-mesenchymal transition of colorectal cancer by miR-153-1. Cancer Manag Res. 2019;11:8699-710.
32. Wang F, Chainani P, White T, Yang J, Liu Y, Soibam B. Deep learning identifies genome-wide DNA binding sites of long noncoding RNAs. RNA Biol. 2018;15(12):1468-76.
33. Liu S, Yang Y, Wang W, Pan X. Long noncoding RNA TUG1 promotes cell proliferation and migration of renal cell carcinoma via regulation of YAP. J Cell Biochem. 2018;119(12):9694-706.

34. Y L, E L, J M, C G, J G, J A, et al. miR-29a suppresses the growth and metastasis of hepatocellular carcinoma through IFITM3. Oncology reports. 2018;40(6):3261-72.
35. P A, S C, C G, P L-P, D L, A K, et al. Identification of the IFITM family as a new molecular marker in human colorectal tumors. Cancer research. 2006;66(4):1949-55.

Supplementary Figure Legend

Supplementary figure 1. A. expression of TUG1 downloaded from the Starbase database. B. The expression of TUG1 and mir-29a in the database. C. Relationship between TUG1 expression and prognosis in the database.D. The relationship between the expression of TUG1 and TNM staging. E. The expression relationship between TUG1 and IFITM3 is shown based on the qRT-PCR results.

Figures

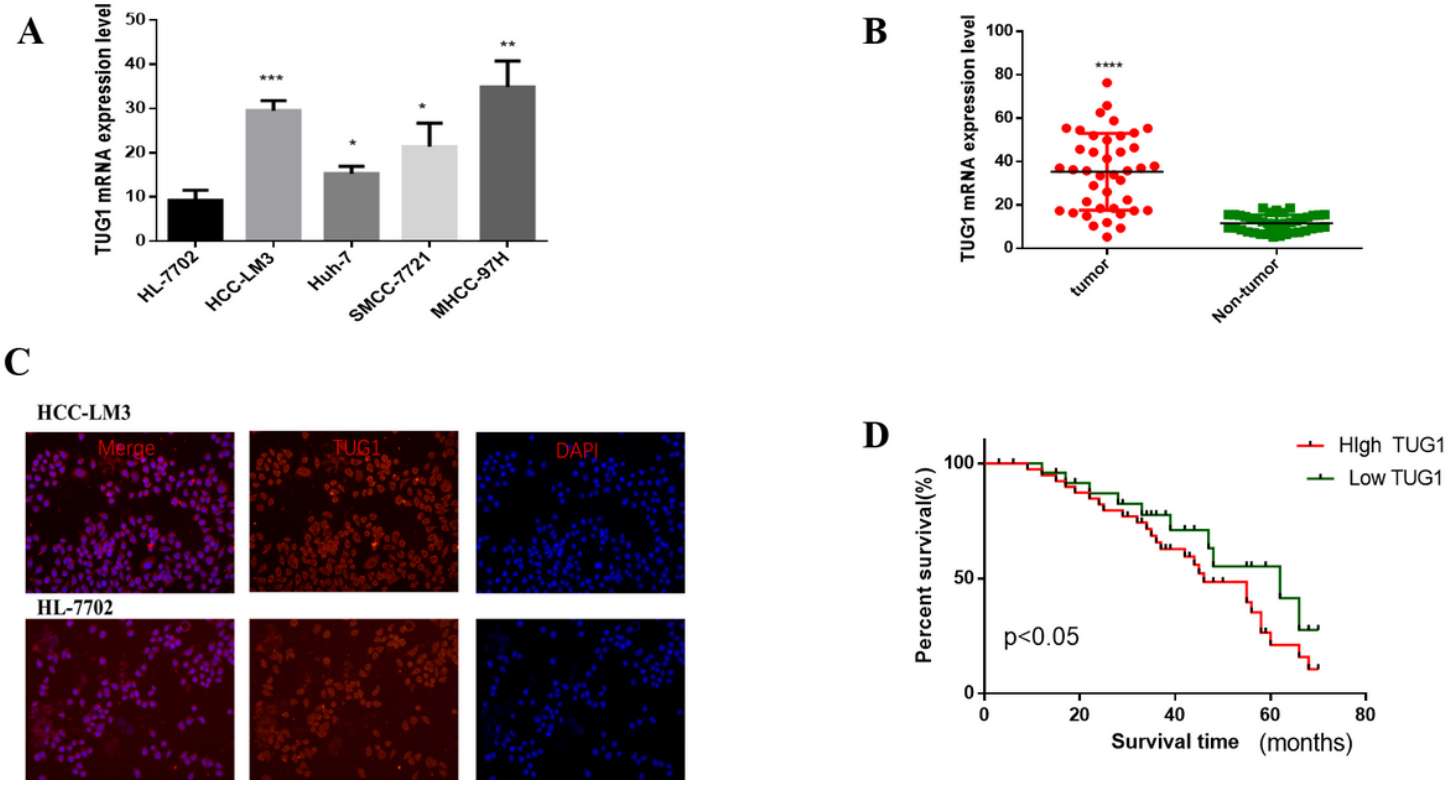

Figure 1

The difference in expression of TUG1 in HCC. A. qRT-PCR was used to detect the expression of TUG1 in HL-7702, HCC-LM3, SMCC-7721, MHCC-97H, and Huh-7 cells. B. qRT-PCR was used to detect the expression of TUG1 in liver cancer tissues and adjacent tissues. C. Immunofluorescence analysis indicated that TUG1 was highly expressed in HCC-LM3 compared with HL-7702 cells,scale bar,200mm. D. The prognosis of patients with high expression of TUG1 was significantly worse than that of patients with low expression ($p < 0.05$). Formula of expression: $2^{-\Delta Ct}$. *$p < 0.05$, **$p < 0.01$, ***$p < 0.001$, ****$p < 0.0001$. The P-value represents the $\chi 2$ test performed to show the difference between the expression of

TUG1 in each group. HCC, hepatocellular carcinoma; AFP, α-fetoprotein; HBsAg, hepatitis B surface antigen; TNM, tumor-node-metastasis; n, number of cases.

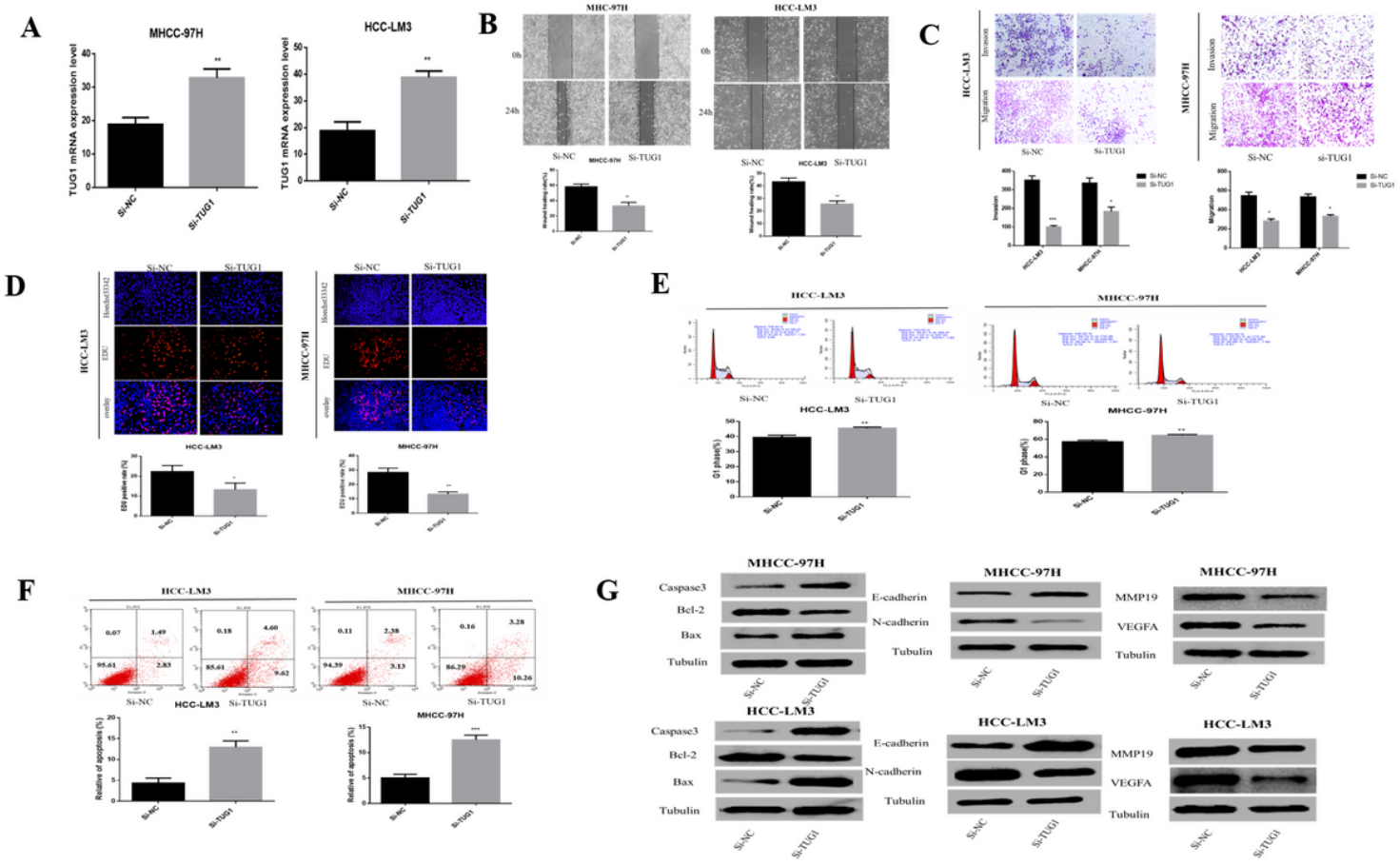

Figure 4

Downregulation of TUG1 can reduce the development of HCC cells. A. The level of TUG1 mRNA after transfection of Si-TUG1 was detected using qRT-PCR. B. Through the wound healing experiments in HCC-LM3 and MHCC-97H cells, the effect of downregulating TUG1 on cell migration ability was observed. C. The migration and invasion abilities of transfected Si-TUG1 to HCC-LM3 and MHCC-97H cells were assessed by Transwell migration and matrix gel invasion assays. D. EdU experiments detected changes in proliferation ability after transfection of Si-TUG1. E. changes in apoptotic rate after Si-TUG1. F. Cyclic changes in HCC cells after Si-TUG1. G. Changes in related proteins after transfection of Si-TUG1. *p < 0.05, **p < 0.01, ***p < 0.001, ****p < 0.0001.

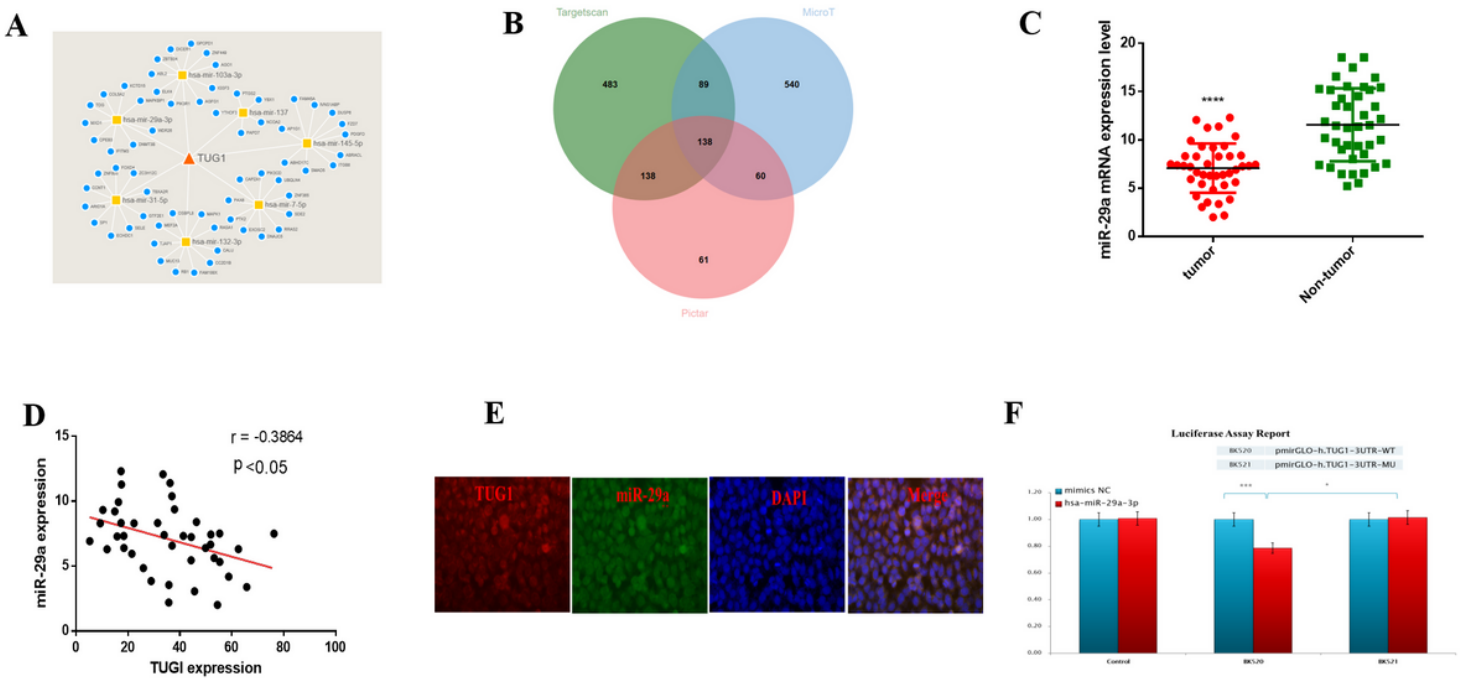

Figure 6

The relationship between TUG1 and miR-29a. A. Multiple databases merged to predict results between TUG1 and downstream genes.B. The downstream target gene of TUG1 was predicted by Venn plot analysis using TargetScan, microT, and Pictar in three ellipses. The target gene was found at the intersection of the three databases. C. qRT-PCR was used to detect the expression of miR-29a in liver cancer tissues and adjacent tissues. D. According to the TUG1 and miR-29a expression diagram. E.the merged images showed that TUG1 and miR-29a are colocalized in HCC tissues using FISH. F. Dual-Luciferase reporter gene assay revealed that TUG1 mimics could reduce the luciferase activities of miR-29a-WT reporter vector rather than miR-29a-MUT, indicating that miR-29a was the targeting gene of TUG1. ($p < 0.05$) * $p < 0.05$, * * * * * $p < 0.01$, $p < 0.001$, * * * * $p < 0.0001$.

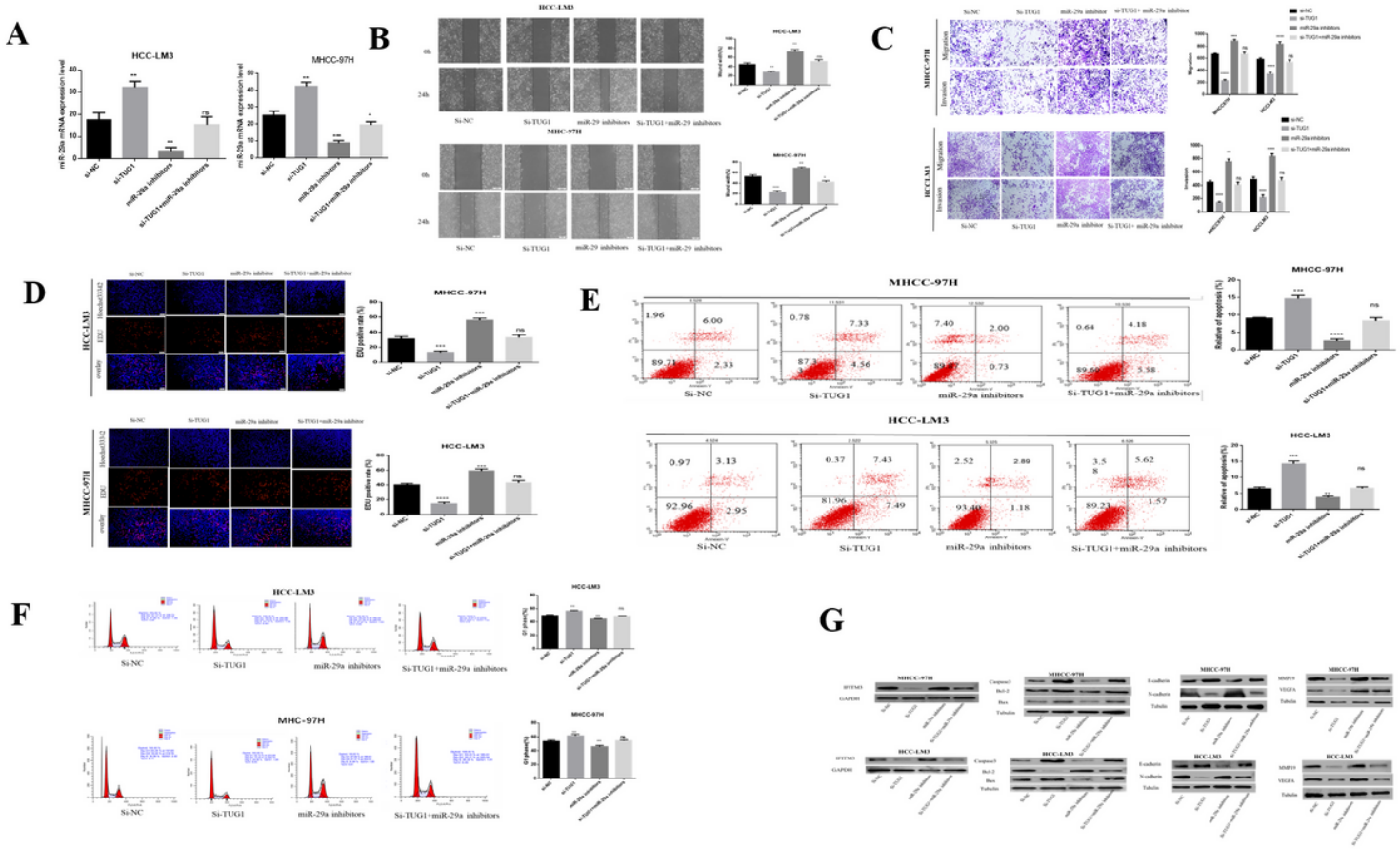

Figure 8

TUG1 inhibits miR-29a expression and promotes migration and invasion of HCC cell lines in vitro. A. qRT-PCR was used to detect the level of miR-29a mRNA after transfection with the Si-TUG1 and miR-29a inhibitors. B. The effects of TUG1 and miR-29a on cell migration ability were observed by wound healing experiments of HCC-LM3 and MHCC-97H cells. C. The migration and invasion abilities of the HCC-LM3 and MHCC-97H cells transfected with Si-TUG1 and miR-29a inhibitors were evaluated by Transwell migration and matrix gel invasion assays. D. EdU assay was used to detect changes in proliferative capacity after transfection of Si-TUG1 and miR-29a inhibitors. E. Changes in the apoptotic rate of Si-TUG1 and miR-29a inhibitors. F. Changes in the cell cycle of Si-TUG1 and miR-29a inhibitors. G. Changes in the expression of related proteins after transfection of Si-TUG1 and miR-29a inhibitors. *p < 0.05, **p < 0.01, ***p < 0.001, ****p < 0.0001.

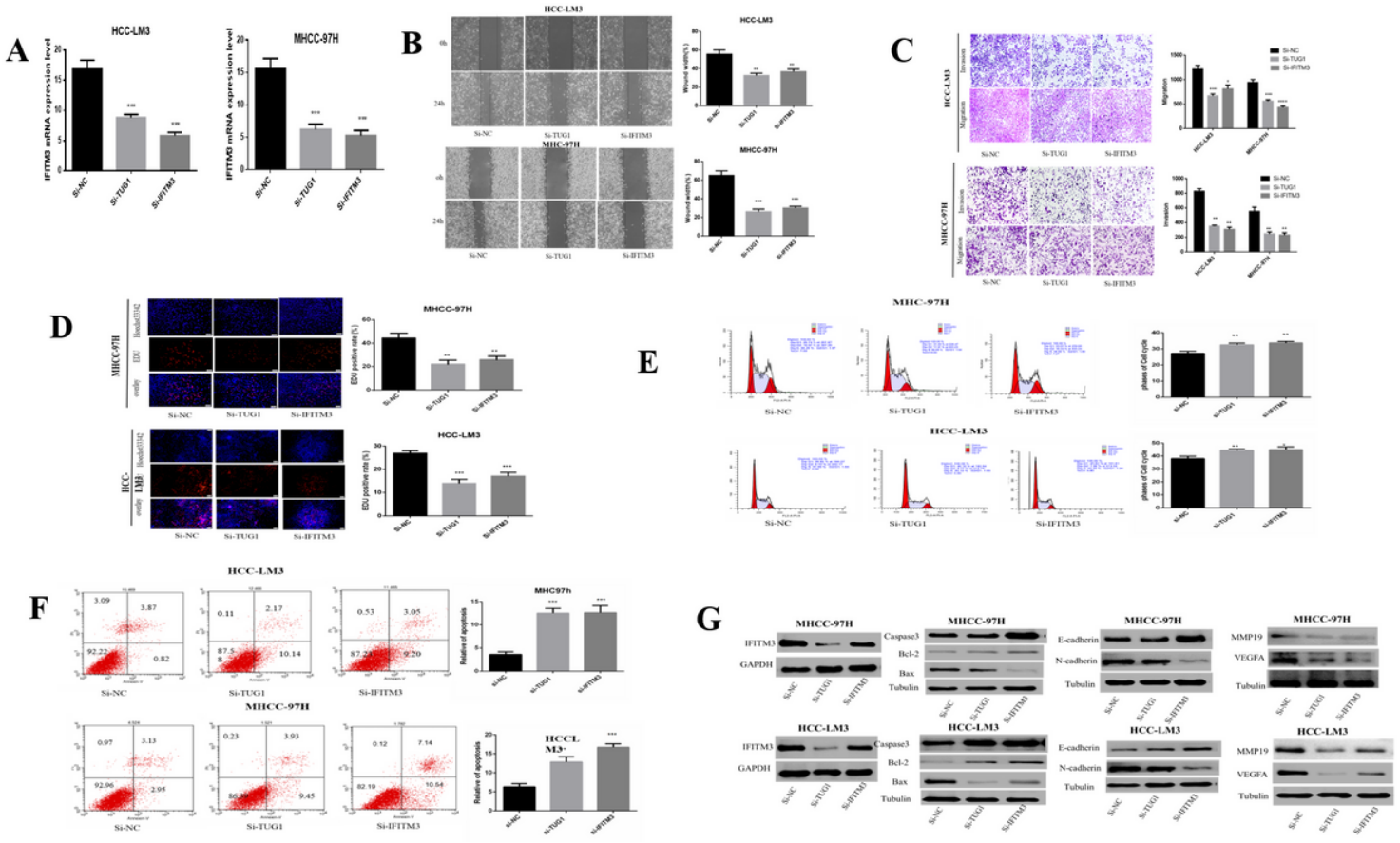

Figure 9

TUG1 regulates IFITM3 expression to promote migration and invasion of HCC cell lines in vitro. A. qRT-PCR detects the level of IFITM3 mRNA after transfection of Si-TUG1 and IFITM3 SiRNA. B. The effects of TUG1 and IFITM3 on cell migration ability were observed by wound healing experiments of HCC-LM3 and MHCC-97H cells. C. The migration and invasion abilities of transfected Si-TUG1 and IFITM3 SiRNA to HCC-LM3 and MHCC-97H cells were evaluated by the Transwell migration and matrix gel invasion assay. D. EdU experiments were used to detect changes in proliferative capacity after transfection of Si-TUG1 and IFITM3 SiRNA. E. Changes in the apoptotic rate of Si-TUG1 and IFITM3 SiRNA cells. F. Transfection of Si-TUG1 and IFITM3 SiRNA cell cycle changes. G. Changes in related proteins after transfection of Si-TUG1 and IFITM3 SiRNA. *p < 0.05, **p < 0.01, ***p < 0.001, ****p < 0.0001.

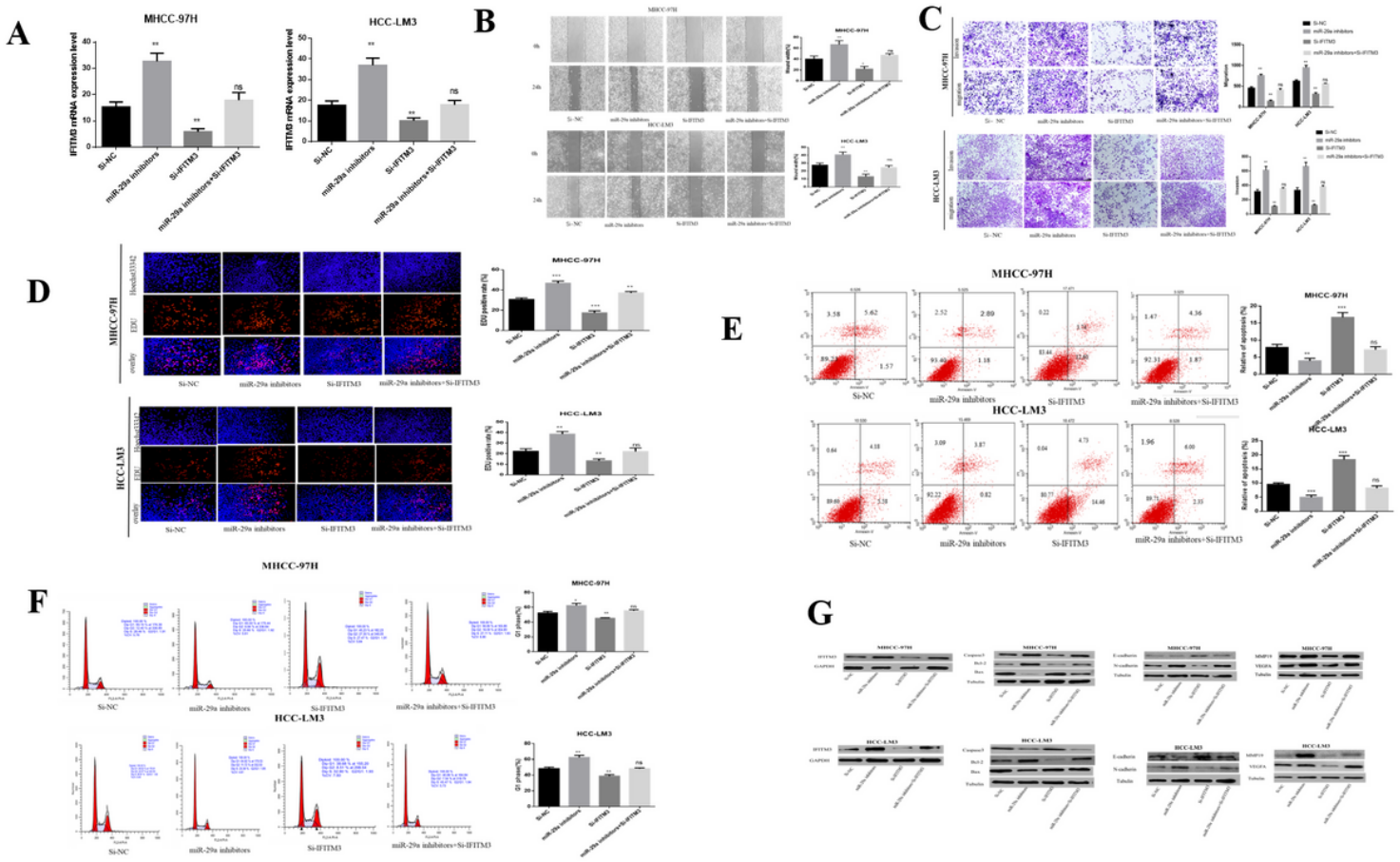

Figure 11

miR-29a inhibits IFITM3 expression, thereby reducing the migration, invasion, proliferation, and apoptosis of HCC cell lines in vitro. A. qRT-PCR was used to detect the level of IFITM3 mRNA after transfection of miR-29a inhibitors and IFITM3 SiRNA. B. The effects of miR-29a and IFITM3 on cell migration ability were observed by wound healing experiments of HCC-LM3 and MHCC-97H cells. C. The migration and invasion abilities of HCC-LM3 and MHCC-97H cells transfected with miR-29a inhibitors and IFITM3 SiRNA were evaluated by the Transwell migration and matrix gel invasion assays. D. EdU assay was used to detect changes in proliferative capacity after transfection of miR-29a inhibitors and IFITM3 SiRNA. E. Changes in apoptosis rate of cells after transfection with miR-29a inhibitors and IFITM3 SiRNA. F. Changes in cell cycle after transfection with miR-29a inhibitors and IFITM3 SiRNA. G. Changes in the expression of related proteins after transfection of miR-29a inhibitors and IFITM3 SiRNA. *p < 0.05, **p < 0.01, ***p < 0.001, ****p < 0.0001.

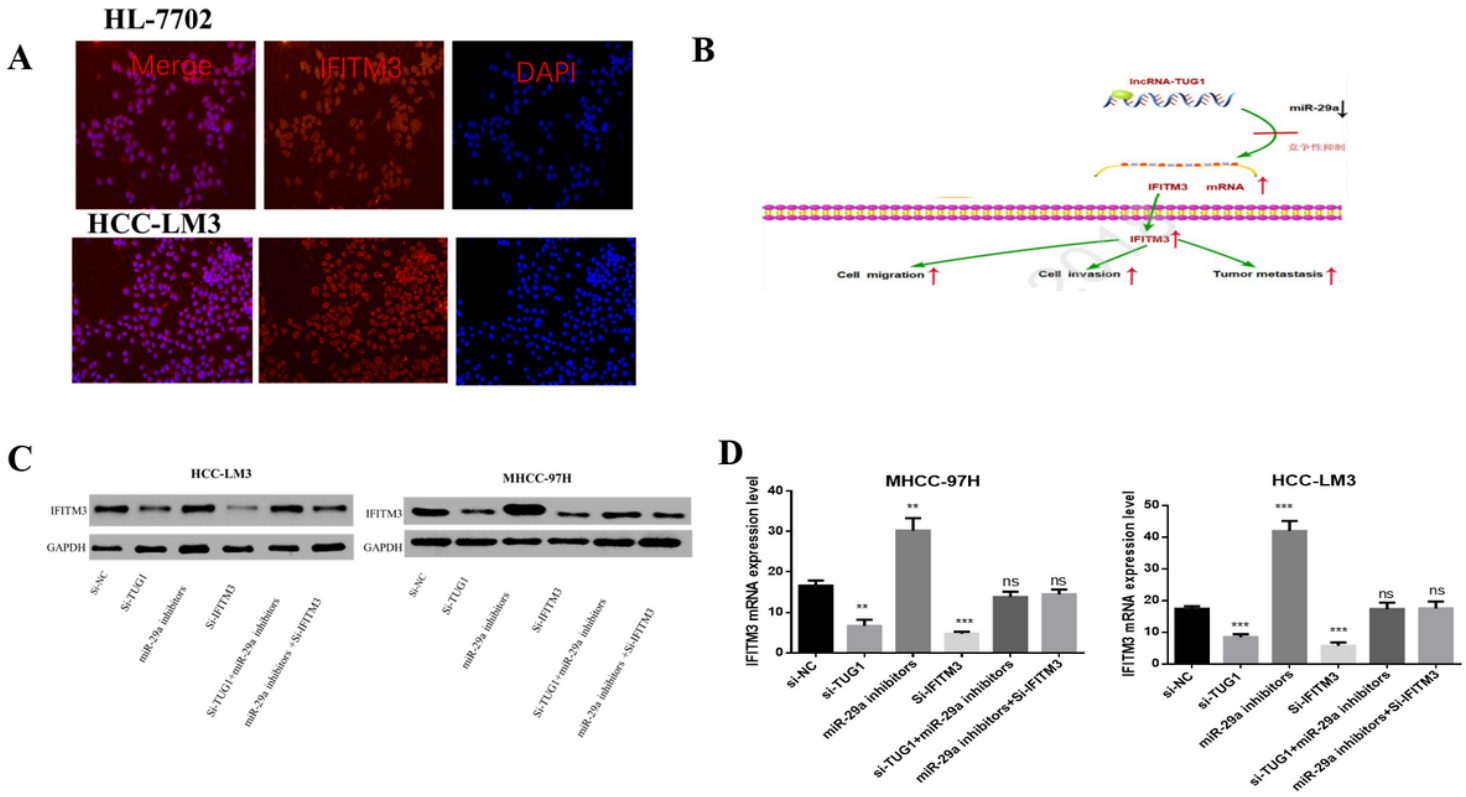

Figure 13

TUG1 promotes the expression of IFITM3 by inhibiting miR-29a. A.The protien level of IFITM3 in HCC-LM3 and HL-7702 were determined by Immunofluorescence, scale bar,200mm. B. TUG1, through inhibition of miR-29a, promotes the expression of IFITM3, which in turn affects the invasion, migration, and proliferation of HCC cells. C. Transfection with TUG1 SiRNA, miR-29a inhibitors, and IFITM3 SiRNA, as well as changes in the expression of related proteins after transfection with TUG1 SiRNA and miR-29a inhibitors, miR-29a inhibitors, and IFITM3 SiRNA. D. Transfection with TUG1 SiRNA, miR-29a inhibitors, and IFITM3 SiRNA and simultaneous expression of IFITM3 mRNA after transfection with TUG1 SiRNA and miR-29a inhibitors, miR-29a inhibitors, and IFITM3 SiRNA. *p < 0.05, **p < 0.01, ***p < 0.001, ****p < 0.0001.

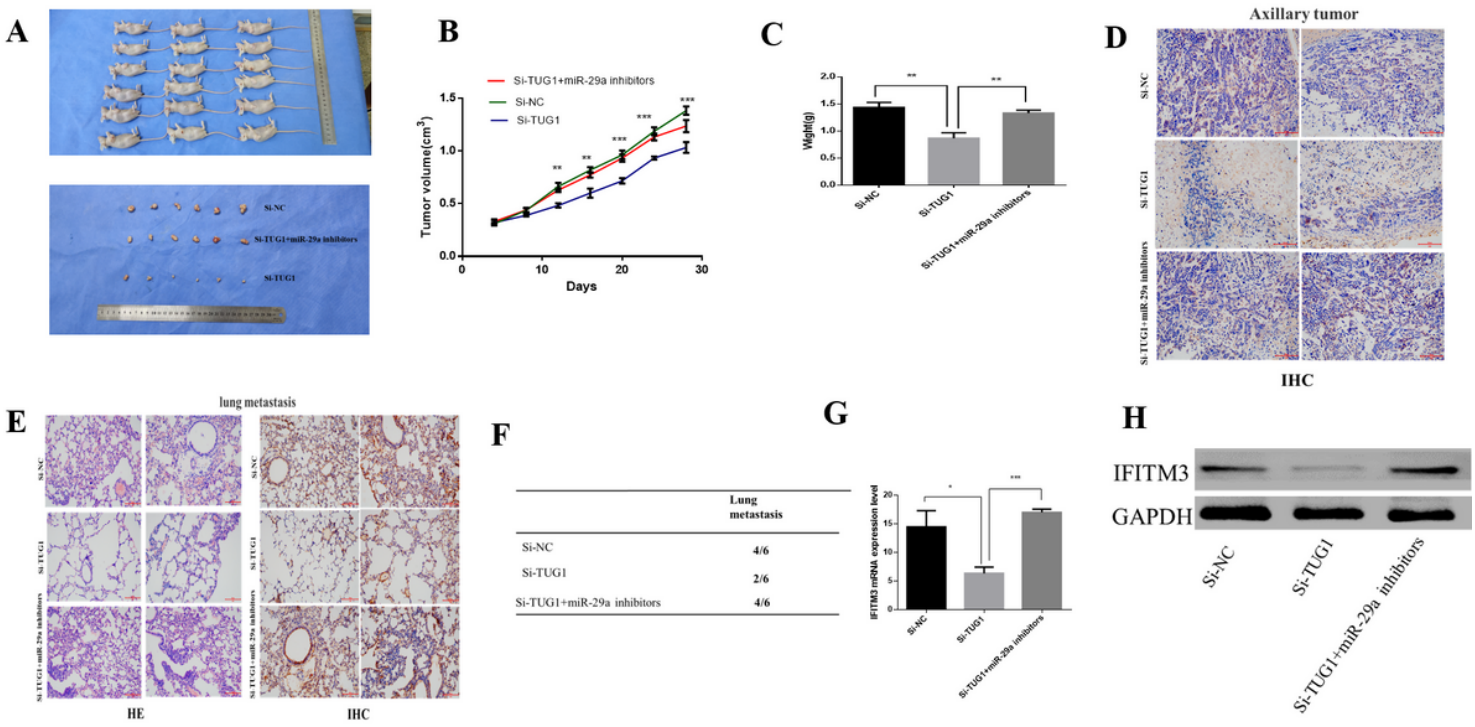

Figure 15

TUG1 regulates miR-29a to promote tumorigenesis in vivo. A. Nude mice were injected with HCC-LM3 stable cells. The tumor was dissected and photographed after 5 weeks. B. Changes in tumor volume of mice were observed every 4 days. C. Mean tumor weight at the end of each group of experiments (Day 28). Data represent the mean SD (n = 6). * P < 0.05. D. Immunohistochemistry was used to detect the expression of subcutaneous tumor IFITM3. E, F, Lung metastasis-related detection. HE staining for histological analysis of lung tissue. Immunohistochemistry to detect the expression of IFITM3 in lung tissue. G, H, Mouse tumors were tested by qRT-PCR and western blotting to detect the expression of IFITM3. *p < 0.05, **p < 0.01, ***p < 0.001, ****p < 0.0001.

Supplementary Files

This is a list of supplementary files associated with this preprint. Click to download.

- Survivalprognosistable.pdf
- Survivalprognosistable.pdf
- Supplementaryfigure1.tif
- Supplementaryfigure1.tif